

Single-domain-wall states in millimeter-scale samples of ErFeO₃L. T. Tsybal,¹ G. N. Kakazei,^{2,3} and Ya. B. Bazaliy^{2,4,*}¹*O. Galkin Donetsk Physics and Technology Institute, NASU, Donetsk 83114, Ukraine*²*Institute of Magnetism, NASU, Kyiv 03142, Ukraine*³*IFIMUP-IN/Departamento de Física, Universidade do Porto, 4169-007 Porto, Portugal*⁴*Department of Physics and Astronomy, University of South Carolina, Columbia, South Carolina 29208, USA*

(Received 30 July 2008; revised manuscript received 2 December 2008; published 20 March 2009)

Hysteresis loops in a $3.9 \times 3.9 \times 3.1$ mm³ single-crystal ErFeO₃ sample were studied in the $4 < T < 70$ K temperature interval. Above and near the compensation point $T_{\text{comp}} = 46$ K the hysteresis loops are rectangular, with the coercive force diverging at T_{comp} . As the temperature is lowered toward the erbium ordering transition at $T_{N2} = 4.1$ K, the shape of the loops experiences a dramatic change. First, the loops develop triangular “tails.” Then the triangles become prominent while the central rectangular part collapses. A double-loop hysteresis pattern with two triangular loops emerges. This behavior is explained by a reversible motion of a single magnetic domain wall in the sample. The simplicity of the magnetic state is related to the small magnetization and correspondingly large domain sizes in orthoferrites. Our model reproduces the correlation of the loops’ shape with the temperature dependence of the total magnetic moment of ErFeO₃.

DOI: [10.1103/PhysRevB.79.092414](https://doi.org/10.1103/PhysRevB.79.092414)

PACS number(s): 75.60.Jk, 75.60.Ej, 75.50.Gg, 75.50.Dd

The process of field-induced magnetization reversal in a ferromagnet is usually hysteretic with the hysteresis loop $M(H)$ produced by the interplay between the crystalline anisotropy of the material, the dipole interaction favoring a magnetic domain structure determined by the sample shape and saturation magnetization, M_s , and the pinning potential. In macroscopic samples with many domains and many pinning centers one normally observes S-shaped irreversible hysteresis loops. Those curves appear smooth, but in fact consist of a large number of infinitesimal magnetization jumps reflecting the motion of numerous domain walls and reversals of microscopic magnetic domains. Accordingly, their shape can be described by Preisach models,¹ based on large ensembles of switching elements. The picture of quasi-continuous reversal by many small jumps can be significantly altered in two cases: (1) magnetic configuration is characterized by only a few domain walls and (2) the pinning potential has a few exceptionally strong centers. In both cases the hysteresis loop can develop a shape with a small number of large jumps separated by continuous reversible segments.

The first case is realized when the size of the sample is comparable to the size of individual domains and therefore only a small number of domain walls, or other defects of magnetic texture, are present. The examples include submicron disks, where the magnetic texture defect is a single magnetic vortex² and nanorings with fractional vortex edge defects.³ Since domain sizes are inversely proportional to the magnetization,⁴ in strong magnets with a large value of M_s the regime of a small number of magnetic defects is achieved only for nanosized particles.

The second case of few strong pinning centers implies that pinning potential is highly nonuniform in space. One would not normally expect that to be the case in a nominally uniform sample; however such a situation can be naturally realized in the presence of a strong surface barrier for the domain-wall creation. An example of such a situation is the domain-wall motion magnetization reversal.⁵ In this case creation of the wall requires the field to be so strong that

other pinning centers become irrelevant and the wall sweeps through the sample as if there was no pinning in the bulk. The magnetization is reversed in one jump and a rectangular hysteresis loop is observed.

In this Brief Report we present a case where both conditions (1) and (2) are satisfied in a millimeter-size rather than a nanometer-size sample. The magnetic state of our relatively large samples is characterized by a small number of domain walls because the material is a weak ferromagnet with low M_s . The orthoferrite ErFeO₃ is a noncollinear antiferromagnet with two magnetic subsystems, one of iron and another of rare-earth ions. Its magnetic properties can be summarized as follows.^{6–8} At Neel temperature $T_{N1} = 636$ K the iron moments order into a canted magnetic structure with antiferromagnetic moment $\mathbf{G} \parallel \mathbf{a}$ and weak ferromagnetic moment $\mathbf{F} \parallel \mathbf{c}$ pointing along the crystallographic axes \mathbf{a} and \mathbf{c} . The erbium ions remain paramagnetic all the way down to helium temperatures. However, they are partially magnetized by the molecular field of the ordered iron ions and acquire an induced magnetic moment \mathbf{m} . The total magnetic moment of the crystal is $\mathbf{M} = \mathbf{F} + \mathbf{m}$. The exchange interaction between Er³⁺ and Fe³⁺ ions is negative,^{6–11} and the erbium moments are pointing opposite to the iron ones partially canceling them. In the temperature interval 88–97 K magnetization \mathbf{M} rotates from the c to a axis. At the compensation point $T_{\text{comp}} \approx 46$ K magnetic moments of two subsystems are exactly equal and $M = 0$. The erbium subsystem orders magnetically at the second Neel transition $T_{N2} = 4.1$ K.^{12–14}

We studied the magnetic hysteresis in ErFeO₃ in the temperature range of 4.2–70 K. Measurements were performed on a $3.9 \times 3.9 \times 3.1$ mm³ single crystal grown by a radiation-induced melting technique. The magnetic moment was measured with a superconducting quantum interference device (SQUID) magnetometer Quantum Design MPMS-5S. Below 88 K the moment is directed along the a axis, and the external field was applied along the same axis, $H \parallel a$ with the accuracy of 3°. Saturation magnetization $M(T)$ was obtained in two ways: (a) by measuring $M(T, H_0)$ in applied “measurement field” H_0 , chosen to produce a single-domain state

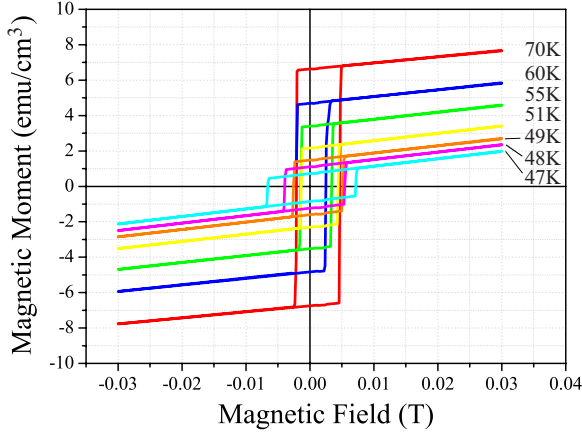


FIG. 1. (Color online) Hysteresis loops in the temperature interval between the spin reorientation transition and the compensation point.

of the sample,¹⁰ and (b) more accurately from the analysis of hysteresis loops $M(H)|_{T=\text{const}}$ at each temperature point. The first method is usually sufficiently accurate and simplifies the measurement procedure. However, correct interpretation of its results relies on the knowledge of the hysteresis loops shapes, as discussed below.

Above and near the compensation point the hysteresis loops $M(H)$ have rectangular shapes (Fig. 1). The coercive force $H_{\text{coerce}}(T)$, defined as the position of the magnetization jump, diverges for $T \rightarrow T_{\text{comp}}$ in accord with previous results.⁹ Here we focus on the shape of hysteresis curves in the temperature region $T < 25$ K (Fig. 2). While they were measured by sweeping the field between ± 3 kOe, only the ± 500 Oe interval containing the loops is shown in the figure. Gradual transformation of the hysteresis curves with temperature is clearly seen. The loop is still rectangular at $T = 23$ K but acquires *triangular tail* shape as the temperature is lowered ($T = 17$ K and $T = 13$ K curves). Then it transforms into a *double-triangle* loop ($T = 9$ K and $T = 5$ K curves). The triangular-tail and double-triangle loops

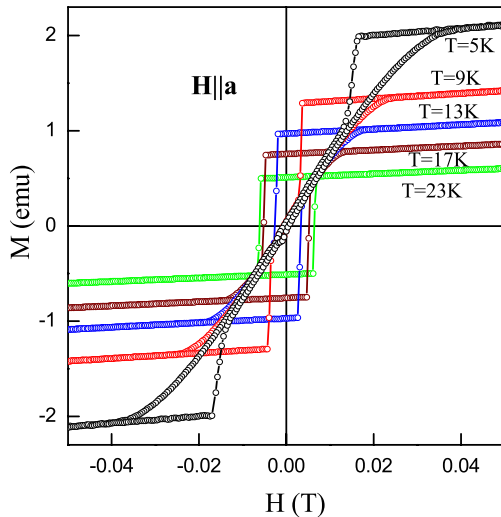


FIG. 2. (Color online) Hysteresis loops $M(H)|_{T=\text{const}}$ in the temperature range $T_{N1} < T < 25$ K.

have three linear branches: the upper and lower branches with small slope and the central branch going through the origin with a large slope. At the saturation field $\pm H_{\text{sat}}(T)$ the central branch joins the upper/lower branches. The magnetization abruptly jumps from upper/lower branches to the central branch at the *jump fields* $H_{\text{jump}(\downarrow/\uparrow)}(T)$, where subscripts \downarrow and \uparrow mark the direction of the jump. The described change in the loop shapes also leads to a peculiar temperature hysteresis of magnetization measured at constant external field.¹¹

We now build a theory for the observed hysteresis curves. Experimentally observed magnitudes of the reversal fields rule out the uniform rotation mechanism which would require a field $H = K/M \sim 10$ kOe, as can be calculated from the known values of anisotropy constant K and magnetization.^{7,9,10} Earlier work¹⁵ has shown that in the case of rectangular loops the reversal is likely to happen through a domain-wall motion process. Here we explain the triangle-tail and double-triangle loops through the same mechanism.

Our main assumption is that the central branch of the loops represents the state of the sample with only two domains separated by a wall. Experimentally, millimeter-size domains were observed optically in another orthoferrite, YFeO₃.¹⁶ Theoretically the domain sizes can be estimated from the results for cubic particles.¹⁷ For $K \gg 2\pi M^2$ (present case) an equilibrium state of a cubic sample of size L is two-domain for $25 \leq L/l_m \leq 75$, where magnetic length $l_m = \sigma/2\pi M^2$ is expressed through the energy σ of the domain wall. The latter is not well known for ErFeO₃, but using the value for TmFeO₃ (Ref. 18) one obtains a condition $0.8 \leq L \leq 2.4$ mm, supporting the two-domain assumption for our sample.

The two-domain magnetic state is fully characterized by the position x of the wall separating the domains. For $|x| < 1$ the wall resides inside the sample, and it is expelled from the sample for $|x| > 1$. In our experiments external magnetic field is small: $H \ll K/M$ and $H \ll H_{\text{eff}}$, where $H_{\text{eff}} \approx 3$ kOe is the effective field characterizing the Er-Fe interaction.⁷ Hence the applied field does not change much the absolute value of magnetization in each domain, and the total magnetic moment can be approximated by $\mathcal{M} = Mx$. Magnetic energy equals

$$E = AM^2x^2 - MHx, \quad (1)$$

where the first term is the demagnetization energy with coefficient A capturing the properties of the sample shape and the second term is the Zeeman energy. Equilibrium position of the wall x_0 is given by $dE/dx|_{x_0} = 0$;

$$x_0(H) = H/H_{\text{exp}}(M), \quad (2)$$

where $H_{\text{exp}} = 2AM$ is the *expulsion field*. While the wall is inside the sample, the pinning of the wall is assumed to be negligible so that the wall follows the energy minimum position $x_0(H)$. Then the central branch is described by

$$\mathcal{M}(H) = Mx_0(H) = H/2A. \quad (3)$$

The no-pinning assumption was checked by the measurements of minor loops for $T \leq 20$ K. The central branch was found to be completely reversible. Furthermore, Eq. (3) is in

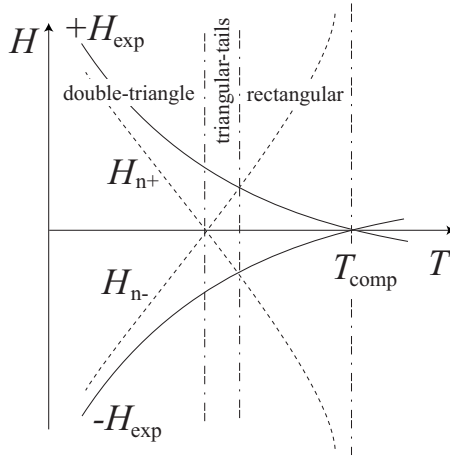


FIG. 3. Theoretical sketch of the temperature dependence of expulsion field H_{exp} (solid curves) and nucleation field $H_{n\pm}$ (dashed curves). Three temperature ranges are formed: with square, triangle-tail, and double-triangle loops.

perfect correspondence with the data in Fig. 2 where the central branch is a straight line $\mathcal{M} \propto H$ with a temperature-independent slope. For a cubic sample the coefficient A can be estimated from the demagnetization factor of a cube as $A \approx N_{\text{cube}} = 2\pi/3 \approx 2.09$. For our sample shape with one shorter side this can be corrected using the approach of Ref. 19 to give an estimate $A \approx 2.42$. With saturation magnetization $M \approx 45 \text{ emu/cm}^3$ at $T=5 \text{ K}$, this would give $H_{\text{exp}} \approx 220 \text{ Oe}$, while the experimental value is about 300 Oe giving a reasonable correspondence with the theory.

At $|H| > H_{\text{exp}}$ the wall leaves the sample which becomes monodomain after that. If the wall is expelled from the sample, there is a barrier for it to get back. The wall must be nucleated, e.g., at the surfaces $x = \pm 1$.²⁰ Consider a nucleation event at $x=1$. The nucleation field H_{n+} required for the wall to enter the sample depends on the pressure $dE/dx|_{x=1} = 2AM^2 - MH$ acting on the wall and the properties of the

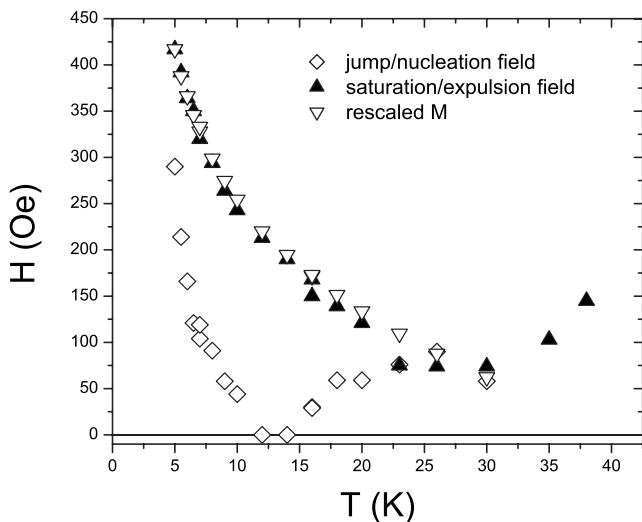


FIG. 4. Experimental temperature dependence of the saturation field $H_{\text{sat}}(T)$ and the absolute value of nucleation field $|H_{n\pm}(T)|$. As predicted by the model, $H_{\text{sat}}(T) \propto M(T)$.

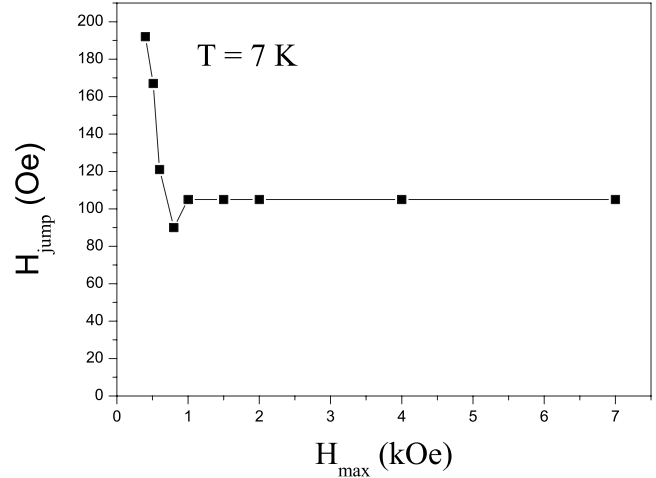


FIG. 5. Jump field dependence on the loop span. The value of H_{jump} is stabilized at large span values.

barrier. Close to the compensation point the magnetization is small and sufficient pressure can be built only at large negative H_{n+} . As one goes away from T_{comp} , the nucleation field remains negative but its magnitude decreases. Due to the demagnetization energy term there is a pressure pushing the wall to enter the sample even at $H \geq 0$ and at sufficiently large values of M the nucleation field becomes positive, $H_{n+} > 0$. In the simplest model of wall nucleation there is a constant barrier $V(x)$ near $x=1$ with characteristic height $V_0 \ll AM^2$ and width $\delta \ll 1$ preventing the wall from entering the sample. The wall can overcome the barrier if the pressure $dE/dx|_{x=1}$ becomes larger than the maximum barrier resistance $(dV/dx)_{\text{max}} \sim V_0/\delta$. This estimate gives an expression

$$H_{n+}(T) = H_{\text{exp}}(T) - \frac{C}{M(T)}, \quad C \sim \frac{V_0}{\delta}. \quad (4)$$

Consider now the hysteresis loop shape. As the field is reduced from the large positive value, the sample remains in the monodomain state with positive magnetization until the wall is nucleated. Two possibilities exist, depending on the value of H_{n+} . If $H_{n+} < -H_{\text{exp}}$, the wall will sweep through the sample and leave it at the other end. A jump of magnetization from $+M$ to $-M$ will be observed, and the resulting loop will be rectangular with $H_{\text{coerce}} = |H_n|$. On the other hand, if $H_{n+} > -H_{\text{exp}}$, the wall will stop at the equilibrium position $x_0(H_{n+})$. In this regime the nucleation field determines the position of the magnetization jump from $\mathcal{M} = +M$ on the upper branch to $\mathcal{M} = Mx_0(H_{n+}) = H_{n+}/2A$ on the central branch. Emergence of a double-loop hysteresis pattern due to a sudden nucleation of an equilibrium domain structure with negligible pinning was previously discussed in the case of thin films²¹ where multiple domain walls were created. In the present case all evidence points to the nucleation of a single wall as discussed in our concluding remarks.

Our theoretical predictions for $H_{n\pm}(T)$ and $H_{\text{exp}}(T)$ are shown in Fig. 3. The loop is rectangular when $H_{n+} < -H_{\text{exp}}$, i.e., near T_{comp} . The triangular tails appear at the point where $H_{n+} = -H_{\text{exp}}$. The double-triangle loop is formed when $H_{n+} > 0$. The saturation field is always equal to the maximum of

expulsion and nucleation fields, $H_{\text{sat}} = \max(|H_n|, |H_{\text{exp}}|)$. In the triangular tails and double-triangle loop regimes $H_{\text{sat}} = H_{\text{exp}} = 2AM$ and hence should be proportional to the magnetization $M(T)$. Experimental values of $H_{\text{sat}}(T)$ and $H_{\text{jump}}(T)$ are plotted in Fig. 4. Overall, the picture corresponds to Fig. 3 and the proportionality $H_{\text{sat}}(T) \propto M(T)$ is maintained with good accuracy. The measured $H_{\text{jump}}(T)$ dependence does not follow Eq. (4) quantitatively but can be fit with 15% accuracy by generalizing to a variable $C(T) \propto (T_{\text{comp}} - T)^2$. In the future, this fit may give a clue about the domain-wall surface nucleation mechanism.

To support the identification of the jump field as the domain-wall nucleation field we measured H_{jump} at $T = 7$ K for variable loop span H_{max} (Fig. 5). Changes in jump field at small spans can be explained by domain-wall pinning at the boundary.²⁰ If the loop span is only slightly larger than H_{sat} , the domain wall may not leave the sample completely, and some magnetization disturbance could be left at the surface. This makes it easier for the domain wall to re-enter and thus creates a positive shift of H_{jump} .

Hysteresis loops in orthoferrites are also known to acquire triangular-tail or double-triangle shapes near the end points of the spin-rotation transition.^{10,22,23} These are very likely to be explained by the same domain-wall motion mechanism. However, a more careful analysis is required since in the

spin-rotation region not only the magnetization but also the domain-wall energies—and so the wall nucleation barriers—exhibit a strong temperature dependence.¹⁸

In conclusion, our experiments and theoretical modeling suggest that millimeter-size samples of ErFeO_3 develop a state with one domain wall in the temperature interval $4 \text{ K} < T < T_{\text{comp}}$. This picture is supported by the following arguments: (a) the shapes of the hysteresis loops are naturally explained by nucleation and reversible motion of a single domain wall. The interplay between the wall nucleation field and the wall expulsion field creates three distinct shapes of the loops, all of which were observed in experiments; (b) the width of the loop is in reasonable correspondence with the calculation for a single domain wall; (c) theoretical estimates of Ref. 17 point to the one wall state; (d) single-wall states were observed in related materials;¹⁶ and (e) positions of the magnetization jumps do not change from one measurement to the other, unlike in the case of many domain walls in Ref. 21. In general, the weak ferromagnetism of the orthoferrites makes them convenient model systems for studying the magnetic states of the nanosized strong ferromagnets.

It is our pleasure to acknowledge illuminating discussions with V. G. Baryakhtar and J. Bartolome.

*yar@physics.sc.edu

¹I. Mayergoyz, *Mathematical Models of Hysteresis* (Springer-Verlag, New York, 1991).

²S. D. Bader, *Rev. Mod. Phys.* **78**, 1 (2006).

³O. Tchernyshyov and G.-W. Chern, *Phys. Rev. Lett.* **95**, 197204 (2005).

⁴A. Hubert and R. Schafer, *Magnetic Domains: The Analysis of Magnetic Microstructures* (Springer-Verlag, Heidelberg, 2000).

⁵E. Kondorsky, *J. Phys. (USSR)* **2**, 161 (1940).

⁶R. L. White, *J. Appl. Phys.* **40**, 1061 (1969).

⁷K. P. Belov, A. M. Kadomtseva, N. M. Kovtun, V. N. Derkachenko, V. N. Melov, and V. A. Khokhlov, *Phys. Status Solidi A* **36**, 415 (1976).

⁸K. P. Belov, A. K. Zvezdin, A. M. Kadomtseva, and R. Z. Levitin, *Orientation Phase Transitions in Rare-Earth Magnetic Materials* (Nauka, Moscow, 1979) (in Russian).

⁹L. T. Tsymbal, Ya. B. Bazaliy, V. N. Derkachenko, V. I. Kameney, G. N. Kakazei, F. J. Palomares, and P. E. Wigen, *J. Appl. Phys.* **101**, 123919 (2007).

¹⁰Ya. B. Bazaliy, L. T. Tsymbal, G. N. Kakazei, A. I. Izotov, and P. E. Wigen, *Phys. Rev. B* **69**, 104429 (2004); Ya. B. Bazaliy, L. T. Tsymbal, G. N. Kakazei, and P. E. Wigen, *J. Appl. Phys.* **95**, 6622 (2004).

¹¹L. T. Tsymbal, Ya. B. Bazaliy, G. N. Kakazei, F. J. Palomares, and P. E. Wigen, *IEEE Trans. Magn.* **44**, 2933 (2008).

¹²W. G. Koehler, E. O. Wollan, and W. K. Wilkinson, *Phys. Rev.* **118**, 58 (1960).

¹³G. Gorodetsky, R. M. Hornreich, I. Yaeger, H. Pinto, G. Shachar, and H. Shaked, *Phys. Rev. B* **8**, 3398 (1973).

¹⁴V. A. Klochan, N. M. Kovtun, and V. M. Khmara, *Zh. Eksp. Teor. Fiz.* **68**, 721 (1975) [*Sov. Phys. JETP* **41**, 357 (1975)].

¹⁵S. Reich, S. Shtrikman, and D. Treves, *J. Appl. Phys.* **36**, 140 (1965).

¹⁶Y. S. Didosyan, H. Hauser, and G. A. Reider, *IEEE Trans. Magn.* **38**, 3243 (2002); Y. S. Didosyan, H. Hauser, G. A. Reider, R. Glatz, and H. Wolfmayr, *J. Appl. Phys.* **93**, 8755 (2003); Y. S. Didosyan, H. Hauser, G. A. Reider, and W. Toriser, *ibid.* **95**, 7339 (2004).

¹⁷W. Rave, K. Fabian, and A. Hubert, *J. Magn. Magn. Mater.* **190**, 332 (1998).

¹⁸F. C. Rossol, *J. Appl. Phys.* **39**, 5263 (1968).

¹⁹M. E. Schabes and A. Aharoni, *IEEE Trans. Magn.* **23**, 3882 (1987).

²⁰R. Allenspach, M. Taborrelli, M. Landolt, and H. C. Siegmann, *Phys. Rev. Lett.* **56**, 953 (1986).

²¹C. Kooy and U. Enz, *Philips Res. Rep.* **15**, 7 (1960).

²²R. Wolfe, R. D. Pierce, S. E. Haszko, and J. P. Remeika, *Appl. Phys. Lett.* **11**, 245 (1967).

²³R. Muralidharan, T.-H. Jang, C.-H. Yang, and Y. H. Jeong, *Appl. Phys. Lett.* **90**, 012506 (2007).